A POSSIBLE MECHANISM OF DYNAMIC AMBIENT OCEAN NOISE HORIZONTAL ENERGY FLOW FORMING

V.A. Shchurov (1), V.P. Dzyuba (1), M.V. Kuyanova (1), A.V. Shchurov (1)

(1) Pacific Oceanological Institute, Far Eastern Branch, Russian Academy of Sciences, 43 Baltiyskaya st., Vladivostok, 690041, Russia

1. INTRODUCTION

The results of experimental investigations of scalar-vector characteristics of underwater ambient noise in deep open ocean in the frequency range of 1-800 Hz are presented here. A telemetric drifting autonomous system with combined receivers was used in the investigations. A combined receiver consisted of a scalar receiver (hydrophone) and a vector receiver of three components particle velocity. The investigation technique is based on simultaneous measurements of pressure P(t) and the particle velocity components $V_x(t)$, $V_y(t)$, $V_z(t)$ at a point of the acoustic field and their a subsequent statistical cross-analysis.

We consider two components of intensity vector $\mathbf{I}(t)\{I_x(t), I_y(t), I_z(t)\}$ the horizontal component $I_{xy}(t)$ and the vertical one I_z (t). Z - axis of vector receiver is directed from the ocean surface to the bottom. The azimuth and the polar angles of the energy flux density vector (intensity vector) are: $\varphi(t)=\arctan(I_y(t)/I_x(t))$, $\vartheta(t)=\arctan(I_{xy}(t)/I_z(t))$. Values $|I_{xy}(t)| = (I^2_x(t) + I^2_y(t))^{1/2}$, $|I_z(t)|$ and angles $\varphi(t)$, $\vartheta(t)$ calculated for some frequency range Δf are value and direction characteristics of ambient noise energy flow in the ocean waveguide over the frequency range Δf.

As it was stressed previously [1-3], ambient dynamic energy flow (in the frequency range of 200-800 Hz) proceeds in two different directions : vertical one (from sea surface roughness to bottom) and horizontal one, coinciding with the direction of wind surface roughness propagation. In this paper the authors examine the temporal dependencies of $\varphi(t)$ and $\vartheta(t)$ for ambient noise energy flow in different frequency over the range of 1-800 Hz and discuss a possible way of forming of a horizontal dynamic noise energy flow, which we revealed and described previously [2]. The measuring facilities and technique are described in [2].

2. TECHNIQUE OF INVESTIGATIONS

Experimental investigations reported here were carried out using telemetric drifting deep-water system transmitting information by a radiochannel to the ship. The general configuration of the combined deep-water eight-channel telemetric system is shown in Fig.1. The telemetric system remained operational at Beaufort wind forces 6. Cancellation of the oscillations arising in the cable line under the effect of the sea surface roughness is performed as follows.

(1) The vertical cable line AB has negative buoyancy of not more than 10-15 kg. This negative buoyancy is compensated for a long chain AC of small floats (lifting capacity of one float is 0.2 kg).

(2) The entire cable line is placed into a vacuum polyurethane plastic "stocking".

(3) The measuring module together with the horizontal cable DE has negative buoyancy with error +0.05 kg. Tilt of the module is not more than +5.

A number of field studies have revealed that the smallest drifting of the measuring system to

A POSSIBLE MECHANISM OF HORIZONTAL ENERGY FLOW

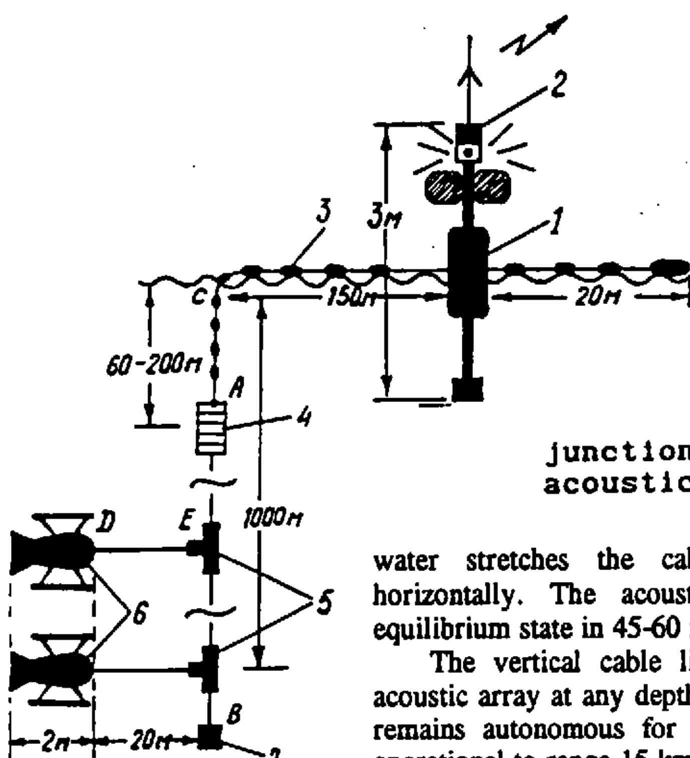

Fig.1. Deployment scheme for the telemetry combined system. The following notation is introduced: 1-container with the apparatus and power supply, 2- radio transmitter, 3 - horizontal cable line with floats, 4- deep water buoyancy, 5- cable junction boxes, 6- combined acoustic module, 7- load

water stretches the cable DE and acoustic module horizontally. The acoustic array restores its working equilibrium state in 45-60 min after setting the system.

The vertical cable line may be connected with the acoustic array at any depth from 20 to 1000 m. The system remains autonomous for 15 days. The Radiotelemetry is operational to range 15 km.

3. RESULTS OF INVESTIGATIONS

The time dependencies of both the azimuth angle φ(t) of noise energy flow horizontal component $I_{xy}(t)$ and the polar angle $\vartheta(t)$ of flux density vector I(t) for eight frequency ranges are shown in Figs. 2-5: 1) 1-5 Hz; 2) 5-12 Hz; 3) 32-64 Hz; 4) 56-112 Hz; 5) 112-141 Hz; 6) 282-355 Hz; 7) 447-562 Hz; 8) 562-800 Hz.

Present the results of noise measurements carried out in the South-Chinese sea. Figs. 2 and 3 show the results obtained in the deployment site at 18°40'N, 115°57'E in May, 89. Conditions of the experiment are as follows: depth - 3600 m; the underwater sound channel axis lies at a depth of 1200 m; the near-surface sound speed is higher than the near-bottom sound speed; wind speed - 12 m/s; steady-state surface roughness, swell; wind waves and swell propagation directions differ by not more then 15°; measuring devices (two combined modules) are mounted at 250 m and 500 m depths; the direction of the combined module axis X coincides with surface wave propagation direction; the combined module axis Z is vertical and directed from the surface to the bottom.

Figs.4 and 5 show the results obtained at the deployment site at 10°53'N, 113°05'E in December, 91. Conditions of the experiment are as follows: depth - 4000 m; the underwater sound channel axis lies at a depth of 1200 m; the near-surface sound speed is higher than the near-bottom sound speed; wind speed - 7 m/s; steady-state surface roughness, swell; wind waves and swell propagation directions differ by not more then 15 ; measuring devices (two combined modules) are mounted at 150 m and 300 m depths.

A POSSIBLE MECHANISM OF HORIZONTAL ENERGY FLOW

For both Figs.2 and 3 the experimental depth was 500 m, for both Figs.4 and 5 it was 150 m. For all frequencies the time of averaging was 120 s. As Figs.2 - 5 show, there are three general directions of ambient noise energy flows in both vertical and horizontal plates. Frequency ranges, corresponding to each direction are: a) 1-12 Hz; b) 32-141 Hz; c) 282-800 Hz.

The polar angles $\vartheta(t)$ for each group are well defined. Noise energy flow in the frequency range of 1-12 Hz (Figs.3, 5) makes an angle between 0° and 30° with the horizontal plane (the angles are measured up from the horizontal plane). Thus the noise energy motion direction in the frequency range of 1-12 Hz in the near-surface layer of the wave guide makes an angle between 0° and 30° with the ocean surface. Consequently acoustic noise sources in this frequency region are placed either on the ocean bottom or within its thickness.

Noise energy flow in the frequency range of 32-141 Hz (Figs.3, 5) makes an angle between 0°and 40° with the horizontal plane (the angles are measured down from the horizontal plane). Hence, the resulting noise energy flow is in the near surface layer of the wave guide and is headed to the underwater noise channel axis. It is well-known that the distant navigation is the noise source in this frequency range.

Noise energy flow vector in the frequency range of 282-800 Hz makes an angle between 0° and 30° with Z axis (according to the extent of surface roughness) as Figs.3, 5 illustrate. It is well-known that the dynamic processes occurring in the near-surface ocean layer are the main noise sources in the frequency range of 200-800 Hz. Our investigations show that the noise energy flow vector in the frequency range of 282-800 Hz makes an angle between 0° and 30° with Z axis (according to the extent of surface roughness), that is, the acoustic noise energy in this frequency range is transported from the surface roughness to the bottom. In this frequency ranges the direction of the energy I_{xy} (t) horizontal component as is shown in [1, 2] coincides with the surface wind roughness propagation direction (wind direction). In the frequency ranges of 447-562 Hz and 562-800 Hz the directions of energy transports in the horizontal plane differ not more than 10° as Fig.2 illustrates. Energy transports proceed inside the angle between 0° and 10°, that is, in directions close to the X axis coinciding with wind speed direction. Fig.4 illustrates the results of the experiment when wind speed direction makes an angle of-(20°-30°) with the X axis. Thus, in this case energy transports occur inside the angle -(10°-30°) in directions close to wind speed direction. In the frequency range 282-355 Hz energy transport coincides with ripple direction. Fig.2 illustrates the situation when the angle between wind wave direction and ripple direction is equal to 10°-15°. In Fig.4 this angle is equal to 20°-30°.

Fig.6 show angular spectra of ambient noise energy flux horizontal component $|I_{xy}(\varphi)|$ for frequency ranges: 282-355 Hz, 447-562 Hz and 562-800 Hz. For all frequencies the time of averaging was 120 s. These angular spectra correspond to Figs.4, 5. They are calculated for time interval from 130 to 250 ss the Fig.4. The maximums of angular spectra show that the main part of noise energy is transferred along two directions, making an angle equal to 30°. Maximums of curves number 2 and 3 correspond a direction of wind wave propagation direction. Maximum of the curve number 1 corresponds ripple propagation direction. The first curve unlike the second and the third ones is asymmetric. The experiment reveals that a stable vertical noise component (in a given frequency region) appears when surface wind speed is 2.0-2.5 m/s. A stable horizontal component of dynamic noise appears when wind speed is 2.5-3.5 m/s and steady-state surface roughness. A value of energy flux horizontal component varies from 1% to 10% of a total energy flux value (and depends on wind speed and the extent of surface roughness). Consequently, we can presume a formation mechanism of horizontal component is connected with processes of redistribution of noise sources initial field on a rough ocean surface.

The time dependence of the azimuth and polar angles of signal energy flow (signal frequency

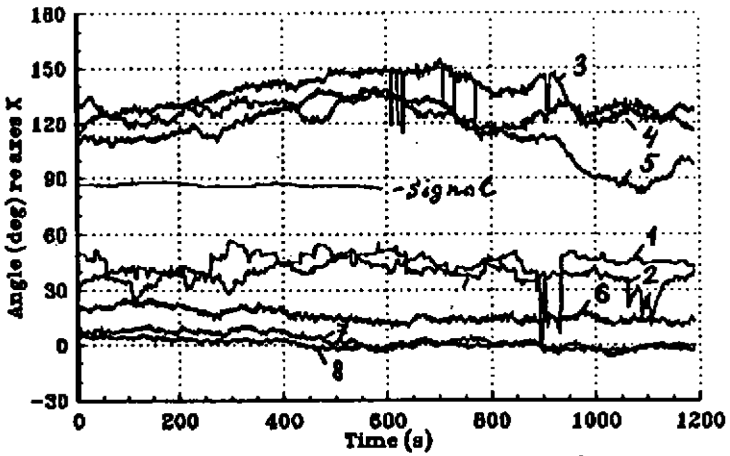

Fig. 2. The time dependence of azimuth angle φ of the noise energy flux vector in the eight frequency ranges. Wind speed is 12 m/s. Experimental depth is 500 m. Exponent averaging time is 120 s. The designations of the frequency ranges are in the text.

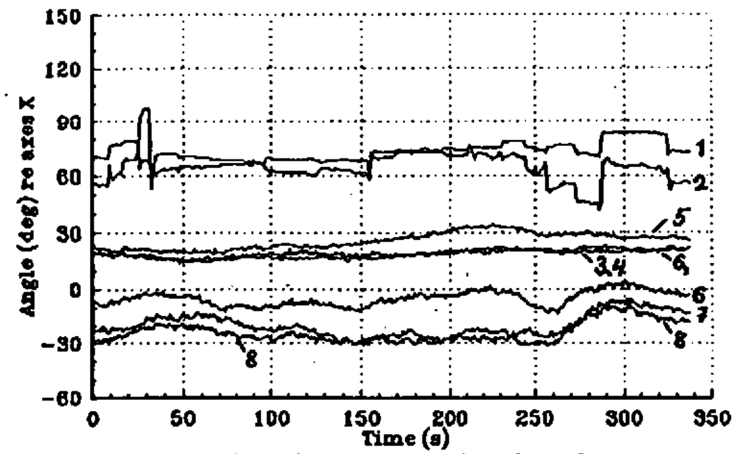

Fig. 4 The time dependence of azimuth angle φ of the noise energy flux vector in the eight frequency ranges. Wind speed is 7 m/s. Experimental depth is 150 m. Exponent averaging time is 120 s.

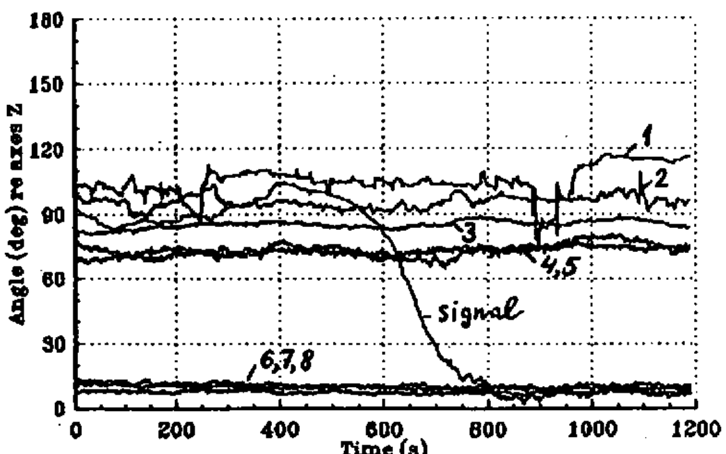

Fig. 3. The time dependence of the polar angle θ of the noise energy flux vector (corresponding to Fig.2).

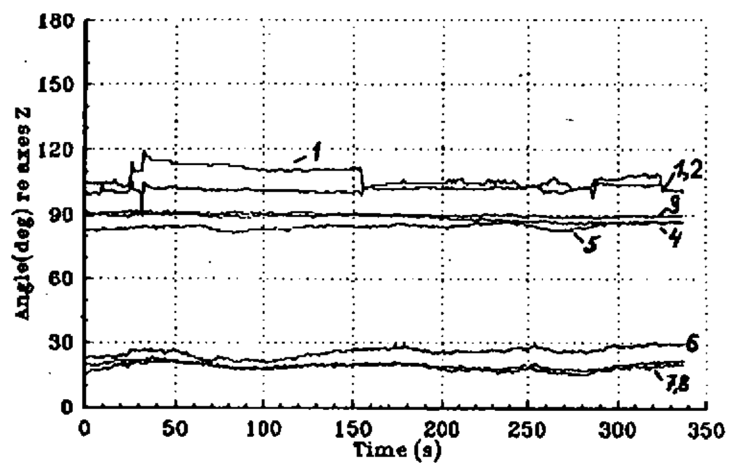

Fig. 5. The time dependence of the polar angle θ of the noise energy flux vector (corresponding to Fig. 4).

is 404 Hz) are shown in Figs. 2, 3. In the pressure spectrum the signal exceeding over the noise is equal to 8-10 dB, in the cross spectrum it is not more then 18 dB. As illustrated in Fig.2, the azimuth angle value remains constant, that is, the acoustic measuring module is motionless in the course of observation. The signal is shut down when t=600 s. In Fig.2 the azimuth angle of 404 Hz signal is not exhibited after t=600 s.

4. THEORETICAL MODEL

As expected in the paper [4-6] re-scattering of the initial acoustic field from the surface roughness is the mechanism of horizontal noise energy flow generation. It is supposed, the character of the initial acoustic field re-scattering in the wind wave propagation direction ("forward") differs from the one in the opposite to the wind wave propagation direction ("backward").The horizontal energy flow value is 0.01-0.1 of the total noise energy flow value (in accordance with the extent of surface roughness) indicating slight differences between mechanisms re-scattering from the surface roughness in the "forward" direction and the "backward" one.

The coincidence of the directions of surface wind wave propagation and horizontal ambient noise energy flux suggests that the anisotropic properties of surface waves give rise to anisotropic properties of noise field in the horizontal plane.

If surface wave propagation direction coincides with the positive +X axis direction, the directions +X and -X are physically different. As to +Y and -Y directions, they can be considered in this case physically equivalent on the average. Hence, the resultant energy flux along the Y axis must be equal to zero which is shown by the experiment, i.e. $\mathbf{I}_{y,n}=\mathbf{I}_{-y,n}-\mathbf{I}_{-y,n}=0$, where $\mathbf{I}_{y,n}=0$ is the averaged resultant noise energy flux component $\mathbf{I}_n$ in the Y direction in certain frequency band; and $\mathbf{I}_{+y,n}$ and $\mathbf{I}_{-y,n}$ are the averaged noise energy flux components in +Y and -Y directions, respectively. The resultant noise energy flux along X axis, as the experiment shows, is not always equal to zero

$$\mathbf{I}_{x,n}=\mathbf{I}_{+x,n}-\mathbf{I}_{-x,n}\neq 0;\ \mathbf{I}_{+x,n}\neq\mathbf{I}_{-x,n}$$

The obtained experimental result can be accounted for by different scattering of the primary noise field of surface sources in the direction of surface wave motion and against it. The magnitude of the resultant noise energy flux in the horizontal plane $\mathbf{I}_{x,n}(f)$ will be proportional to the difference of sound scattering coefficient $\Delta m(\theta)$ in the +X and -X directions and the energy flux value

$$\mathbf{I}_{x,n}\approx\Delta m(\theta)\mathbf{I}_n(f),$$

where θ is the local angle of the sound incident on surface. For a slight sea roughness one can write

$$\Delta m(\theta)\approx(\partial m(\theta)/\partial\theta)\Delta\theta.$$

For a large-scale sea roughness, we obtain the following frequency function (at small sliding angles)

$$\mathbf{I}_{x,n}(f)/\mathbf{I}_n(f)=\gamma_{pVx(f)},\ \gamma_{pVx}(f)\sim(\partial m(\theta)/\partial\theta)\Delta\theta,$$

which agrees well with the experiment.

The main part of the horizontal flow is caused by sound wave directed under small sliding angles to the ocean surface. Under these conditions method of small perturbation (MSP) may be used for large-scale roughness too. To a first approximation of MSP an average intensity of the scattered field I_s is [7]:

A POSSIBLE MECHANISM OF HORIZONTAL ENERGY FLOW

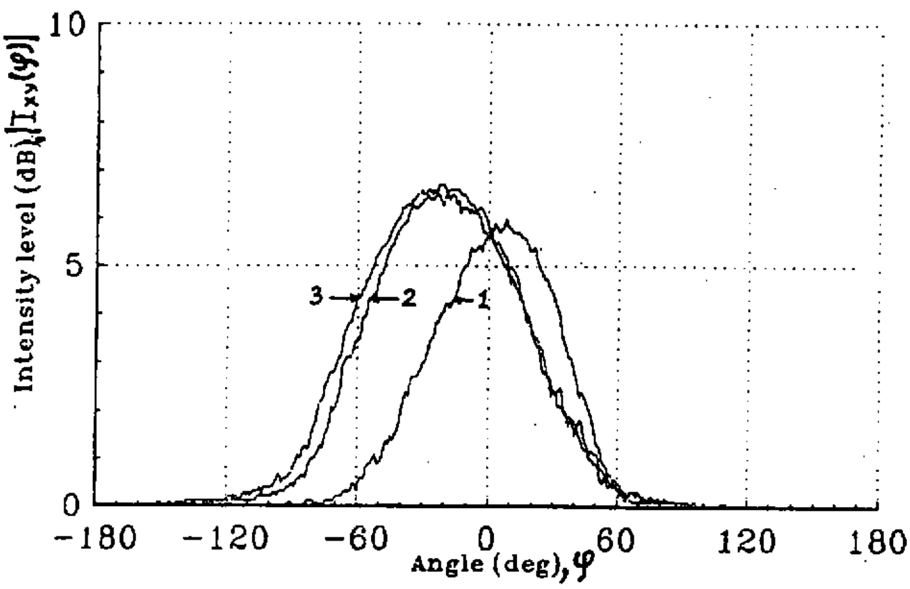

Fig. 6. Angular spectrum of ambient noise energy flux I_{xy} .Frequency ranges 1-282-355 Hz; 2-447-562 Hz; 3-562-800 Hz; X axes corresponds 0° angle and Y axes does 90°. The time of averaging is 120 s; X, Y are the combined receiver axes.

$$I_s = 4\int_{\Gamma} I(\theta_o,\varphi_o)k_z^2 G(\bar{\chi})d\bar{\chi},$$

where $I(\theta_o,\varphi_o)$ is the intensive of sound radiation incident under angles θ_o,φ_o, k_z is its vertical wave number, $G(\bar{\chi})$ is two-scale spatial spectrum of the surface roughness. The wave vectors of scattered field $\bar{k}_s$, incident field $\bar{k}_o$ and spatial spectrum of roughness $\bar{\chi}$ are connected by Bragg's law:

$$\bar{k}_s = \bar{k}_o + \bar{\chi}$$

The flow along X - axis is summarised by the waves with projections $k_s^x \geq 0$.
From this condition and Bragg's law it follows that $-k \leq \chi^x \leq k$, were $k=2\pi/\chi$.

If $k_o^x \leq 0$, than $-k \leq \chi^x \leq 2k$.
In a similar manner, for the flow in the opposite direction we have: $-2k \leq \chi^x \leq k$.
The resultant flow along X - axis is:

$$I_{x,n} = I_{+s}\cos\varphi_+\sin\theta_+ - I_{-s}\cos\varphi_-\sin\theta_-,$$

where φ_+, φ_-, θ_+, θ_- are the average scatter angles along and opposite X - axis. If sound propagates in vertical plane XOZ ($\varphi=0$) than with consideration for sliding scattering we have:

$$I_{x,n} = I_{+s} - I_{-s} = 4\int_{-k}^{2k} I(\theta_o,0)k_z^2[G(\chi_x)-G(-\chi_x)]d\chi_x.$$

A POSSIBLE MECHANISM OF HORIZONTAL ENERGY FLOW

The coherence function giving regard to uniformly directed incident radiation is:

$$\gamma_{pV_x}(f) = \frac{2}{\pi}\int_{-k}^{2k} k_z^2\,[G(\chi_x)-G(-\chi_x)]\,d\chi_x.$$

where $2\pi f = k \cdot c$, c is sound velocity.

Last equation shows that in limits of MSP there is a simple connection of measured characteristics of the acoustic field $\mathbf{I}_{x,n}$ and γ_{pV_x} with the spatial spectrum of roughness. And this connection may be used for determining of $G(\bar{\chi})$.

In this manner we can arrive a direct correlation between energy flux $\mathbf{I}_{x,n}$ and surface roughness $G(\bar{\chi})$ spatial spectrum. Using $\mathbf{I}_{x,n}$, γ_{pV_x} obtained from acoustic measurements we can make an estimate of spectrum $G(\bar{\chi})$. This method can be useful because the direct measurement of the spatial spectrum of the wind waves in the open ocean meets some technical difficulties.

5. REFERENCES

[1] V.I. ILYICHEV, V.A. SHCHUROV, V.P. DZYUBA & V.P. KULESHOV, "Investigation of the acoustic noise field in the ocean using vector-phase methods", Akustika Okeanskoy Sredy, edited by L.M.Brekhovskikh and I.B.Andreyevoi (Nauka, Moscow, 1989), pp.144-152 (in Russian)

[2] V.A. SHCHUROV, "Coherent and diffusive fields of underwater acoustic ambient noise", J.Accost.Soc.Am. Vol.90, No.2, Pt. 1, August 1991, pp. 991-1001.

[3] А.И. ВЕЛИЧКО, В.Е. ИВАНОВ, С.А. ИЛЬИН, В.А. КИРШОВ, А.С. НЕСТЕРОВ "Угловые характеристики шумов океана в инфразвуковом диапазоне частот", Сб. научных трудов "Модели и алгоритмы построения систем и комплексов обработки акустической информации", Ленинград, Россия, 1990, с.144-148.

[4] V.A. SHCHUROV, "Ambient noise energy motion in the near-surface ocean layer", Recent Advances in Underwater Acoustics, Proc.I.O.A. Vol 13, Part 3 (1991), Weymouth, UK, pp. 250-256.

[5] V. SHCHUROV, V. ILYICHEV & YU. KHVOROSTOV "Ambient noise anisotropy in horizontal plane", Proc. ICA-14, E1-10, (1992), Beijing, China

[6] V.A. SHCHUROV et al. " The ambient noise energy motion in the near-surface in ocean wake-guide", Journal de Physique IV, Colloque C5, supplement au Journal de Physique III, volume 4, mai 1994, France, C-1273.

[7] L. BREKHOVSKIKH, YU. LUSANOV "Fundamentals of Ocean Acoustics", Spinger-Verlag Berlin Heidellerg New York 1982.